DMD Fast Forward. Published on October 2, 2013 as doi:10.1124/dmd.113.053876

Modulation of the UGT2B7 Enzyme Activity by C-Terminally Truncated Proteins Derived from Alternative Splicing

Vincent Ménard, Pierre Collin, Guillaume Margaillan and Chantal Guillemette

Pharmacogenomics Laboratory, Centre Hospitalier de l'Université Laval de Québec (CHU de Québec) Research Center and Faculty of Pharmacy, Laval University, Québec, Canada (V.M., G.M., P.C. and C.G.). Canada Research Chair in Pharmacogenomics (C.G.).

Running title: *UGT2B7 alternative regulatory proteins*

Correspondence to Chantal Guillemette, Ph.D., Canada Research Chair in Pharmacogenomics, Pharmacogenomics Laboratory, CHU de Québec Research Center R4720, 2705 Boulevard Laurier, Québec, Canada, G1V 4G2, Tel. (418) 654-2296; Fax (418) 654-2279; E-mail: chantal.guillemette@crchul.ulaval.ca

Total number of text pages: 30

Words number:

Abstract: 249

Introduction: 752

Discussion: 1303

Number of references: 48

Number of figures: 8

Number of supplemental figures: 1

Number of tables: 0

Number of supplemental table: 1

Abbreviations: UGT: UDP-glucuronosyltransferase, AZT: zidovudine

ABSTRACT

The enzyme UGT2B7 is one of the most active UDP-glucuronosyltransferases (UGTs) involved in drug metabolism and in maintaining homeostasis of endogenous compounds. We recently reported the existence of 22 *UGT2B7* mRNAs, two with a classical 5' region but alternative 3' ends namely UGT2B7_v5 (containing a novel terminal exon 6b) and _v7 (exon 5 excluded) that encode enzymatically inactive isoforms 2 (i2) and i4, respectively. The v1 mRNA encoding the UGT2B7 enzyme (renamed isoform 1 or i1) is co-expressed with the splice variants v5 and v7 in human liver, kidney, and small intestine and the hepatic cell lines HepG2 and C3A. The presence of alternate v5 and v7 transcripts in isolated polysomes from these hepatic cells further supports endogenous protein translation. Cellular fractionation of clonal HEK293 cell lines overexpressing UGT2B7 isoforms demonstrates that i1, i2 and i4 proteins co-localize in the microsomal/Golgi fraction, whereas i2 and i4 can also be found in the cytosol; a finding sustained by immunofluorescence experiments using tagged proteins. Then, by modifying splice variant abundance in overexpression in HEK293 and HepG2 cells as well as RNA interference experiments in HepG2 and C3A cells, we observe drug glucuronidation phenotypes compatible with variant-mediated repression of UGT2B7 activity without consequent alteration of the apparent enzyme affinity (K_m). Finally, co-immunoprecipitation experiments support a direct protein-protein interaction of i2 and i4 proteins with the functional UGT2B7 enzyme as a potential causative mechanism. These findings point towards a novel auto-regulatory mechanism of the UGT2B7 glucuronidation pathway by naturally occurring alternative i2 and i4 proteins.

INTRODUCTION

Alternative splicing has been documented for more than 95% of multi-exon human genes and is responsible for transcriptome expansion and protein diversity (Pan et al., 2008). This post-transcriptional mechanism has been reported for genes involved in drug metabolism, most notably cytochromes P450 (CYPs) (Turman et al., 2006), sulfotransferases (He et al., 2005), glutathione S-transferase (Ross and Board, 1993), and UDP-glucuronosyltransferases (UGTs) (Levesque et al., 2007). UGT1A family members are derived from the use of alternative promoters and exons 1, while *UGT2B7* is subjected to extensive alternative splicing (Innocenti et al., 2008; Guillemette et al., 2010; Menard et al., 2011).

UGT2B7 is an enzyme responsible for detoxification of xenobiotics including drugs such as morphine, efavirenz, zidovudine, and fenofibric acid, and is involved in the homeostasis of endogenous molecules like eicosanoids, bile acids and sex steroids (Jin et al., 1997; Barbier et al., 2000; Stone et al., 2003; Turgeon et al., 2003; Thibaudeau et al., 2006; Mano et al., 2007; Belanger et al., 2009; Tojcic et al., 2009; Trottier et al., 2013). Its expression is high in liver and kidney, but also detectable in the gastrointestinal tract and peripheral tissues (Nakamura et al., 2008; Court et al., 2012). The *UGT2B7* gene is located on chromosome 4q13, has 6 classical exons and spans 17kb (Mackenzie et al., 2005). As for discoveries related to alternative splicing of this gene, two additional distal 5' exons were initially observed (referred to as exons 1a and 1b, respectively, and located 44 kb and 7 kb from the classical translation start site in exon 1) (Innocenti et al., 2008). Our group then uncovered two additional 5' exons (1c and 1d, situated between exon 1a and 1b) as well as two novel 3' exons (6b and 6c, located in the intron between exon 5 and the classical exon 6, renamed 6a) (Menard et al., 2011). Alternative splicing at the

UGT2B7 locus produces at least 22 full-length transcripts mainly observed in kidney and liver. Consequently, the UGT2B7 enzyme has been renamed isoform 1 (i1) and is encoded by the variant transcript 1 (v1). The variant *UGT2B7* mRNAs potentially encode six shorter proteins with variable N-terminal and/or C-terminal ends that were named i2 to i7. Whether these alternative proteins are biologically active remains to be demonstrated.

Recent observations related to alternative splicing of the UGT1A family members revealed nine variant proteins derived from the use of an alternative 3' exon (5b) with a shorter C-terminal end (named isoforms 2 or i2s) that regulate UGT1A-mediated glucuronidation by UGT1A enzymes (or i1s) (Girard et al., 2007; Levesque et al., 2007). Indeed, UGT1A_i2s are enzymatically inactive but repress glucuronidation through protein-protein interactions with active UGT1A_i1s (Bellemare et al., 2010b). Data suggest that interactions between isoform 1 and 2 proteins lead to an inactive complex and that i2 proteins decrease rates of glucuronide formation without affecting the kinetic model and substrate binding (Bellemare et al., 2010a). The oligomeric nature of UGT proteins has been known for some time: for UGT2B7, homodimerization is suspected to lead to atypical enzyme kinetics for certain substrates that is best described by a two-sites model (Lewis et al., 2011), whereas heterodimerization can occur with several other UGT proteins and CYP enzymes resulting in altered activity (Fremont et al., 2005; Fujiwara et al., 2010).

Two *UGT2B7* splice variants have a classical 5' region but have an alternative terminal exon 6b (variant 5 or v5) or a deletion of the exon 5 (variant 7 or v7), sharing similarities to UGT1A activity-modulating splice variants (Menard et al., 2011). While the UGT2B7 enzyme (i1) is derived from transcript v1, transcripts v5 and v7 encode C-terminally truncated i2 and i4 proteins,

respectively. Here we sought to characterize their modulatory potential on cellular glucuronidation. We initially tested various commercial sources of UGT2B7 antibodies with the aim of assessing expression of UGT2B7 isoforms in cellular models and human tissues. We then evaluated the effect on glucuronidation kinetics of stably co-expressing i2 and i4 proteins along with the UGT2B7 enzyme as well as their subcellular localization by immunofluorescence and western blotting of centrifugation fractions. Then, we tested the influence of partial depletion of endogenous UGT2B7 variants and their overexpression on glucuronidation activity of two human liver cell lines, HepG2 and C3A. Lastly, co-immunoprecipitation experiments allowed us to test the possibility of a direct protein-protein interaction of i2 and i4 proteins with the functional UGT2B7 enzyme. Our findings support that truncated UGT2B7 i2 and i4 variant isoforms have inhibitory properties *in vitro* and may contribute in the control of UGT2B7-mediated glucuronidation.

MATERIALS AND METHODS

Cellular Models. HepG2, HEK293 and C3A (ATCC, Rockville, MD, USA) were cultured as recommended with 10% fetal bovine serum. HepG2 is derived from a hepatocellular carcinoma and C3A is a clonal derivative of HepG2 that exhibits a better differentiated hepatic phenotype (Filippi et al., 2004). The cloning of UGT2B7_v1, v5, and v7 cDNAs encoding UGT2B7 i1, i2, and i4 proteins and methodologies for transfection of HEK293 cells to produce stable clones have been described (Menard et al., 2011). Briefly, prior to antibiotic selection, cells were grown for 48 h and then transfected with 5 µg of DNA by electroporation using the Neon Transfection System (Life Technologies, Carlsbad, CA, USA). For expression in HepG2 cells, plasmid constructs containing v5 and v7 with or without a V5 epitope were transfected as well as an empty pcDNA6 acting as a mock control. For RNA interference experiments, two short interfering RNAs (siRNAs) were purchased from Thermo Scientific (Waltham, MA, USA): one directed against the exonic end and the proximal 3'-untranslated region of the exon 6b (5'-ctgctaaactgtcttccaa-3') and the other against the ex4–ex6a splicing event (5'-ccttctagatataaagaga-3'). Specificity of siRNAs was tested using BLAST (http://blast.ncbi.nlm.nih.gov/). A negative control was also purchased from Thermo Scientific (ON-TARGETplus Non-targeting siRNA #3). After transfection with siRNA, cells were grown for 48 h without antibiotics and then harvested. Cell lysates were prepared for glucuronidation assays and western blotting. Total RNA was extracted with Tri-Reagent (Sigma-Aldrich, St. Louis, MO, USA) for use in quantitative real-time PCR.

Western Blotting and Glucuronidation Assays. Microsomes and cell lysates were prepared as described (Lepine et al., 2004). The protein concentrations were determined using the BCA

protein assay (Fisher Scientific, Ottawa, ON, Canada). Polyclonal antibodies against UGT2B7 from Millipore (Billerica, MA, USA), BD Gentest (Franklin Lakes, NJ, USA), and Abcam (Cambridge, UK) were tested for specificity using 20 µg of microsomes of HEK293 clones overexpressing each of the UGT2Bs, following the manufacturers' protocols**.** A non-selective anti-UGT2B, called EL-93, was produced in-house (Guillemette et al., 1997) and used as a positive control of UGT overexpression. Glucuronidation assays on AZT (3'-azido-3'-deoxythymidine from Sigma-Aldrich) were performed using microsomes (20 µg) or homogenates (50 µg), and glucuronides (-G, e.g., AZT-G) were detected by a mass spectrometry–based assay as described (Thibaudeau et al., 2006; Belanger et al., 2009). Kinetic parameters of glucuronidation were assessed in assays containing a 100–5000 µM range of AZT. Kinetic parameters were estimated using Prism 6 (http://www.graphpad.com). Densitometric measurements of the UGT2B7 enzyme (i1) protein levels by western blotting served to normalize glucuronidation activity. Briefly, microsomes isolated from cells used in the enzyme kinetics, siRNA and overexpression experiments were blotted and revealed using the anti-2B7 from Millipore. Western blotting with a monoclonal antibody directed against the V5 epitope further revealed the presence of i1 proteins in HEK293 membranes upon overexpression. The relative levels of i1 proteins were assessed by integrated optical density using the Bioimage program Visage 110S (Genomic Solution Inc., Ann Arbor, Michigan, USA), and activity levels were normalized by these values. Statistical significance was evaluated by a paired Student's t test ($p < 0.05$) using XLSTAT for Mac (xlstat.com).

Gene Expression Profiling by Quantitative Reverse Transcription PCR (qRT-PCR) in UGT2B7-depleted Cells. Total RNA from adult human tissues was purchased from Life

Technologies (Carlsbad, CA). cDNA was synthesized with 1 µg of RNA and 250 ng of random hexamers with Superscript III reverse transcriptase (Life Technologies) following the manufacturer's protocol. RT-PCR amplification of full-length transcripts was done as described (Menard et al., 2011) using primers described in **Supplemental Table 1**. Real-time quantitative PCR (qPCR) assays were performed in triplicate in a StepOne real-time PCR system with the Sybr Green PCR master mix (Life Technologies), 12 ng of cDNA, and 500 nM of primers designed to specifically amplify the ex5-ex6b and ex4-ex6a splicing events specific to variant v5 and v7, respectively. Amplification of the ex5-ex6a splicing event, a splicing event characteristic of the active enzyme, was used as a control of the specificity of the siRNAs used herein. Results were normalized according to *RPLP0* (36B4) gene expression. All primers used for qRT-PCR amplifications are detailed in **Supplemental Table 1**. During qRT-PCR optimization, five different concentrations of vectors containing v1, v5, v7, and 36B4 were used to delineate standard amplification curves, and expression data are reported as the number of AS events per 10,000 36B4 copies.

Immunofluorescence. HEK293 clones stably expressing UGT2B7 fusion proteins i1-V5, i2-V5, and i4-V5 were used to visualize the V5 epitope (mouse monoclonal anti-V5, Life Technologies; 1:100), the endoplasmic reticulum (ER)-specific protein calnexin (rabbit polyclonal anti-calnexin, Enzo Life Sciences, Farmingdale, NY, USA; 1:200) and the Golgi-specific protein giantin (rabbit polyclonal anti-giantin, Abcam; 1:2000) in immunofluorescence experiments. Two secondary fluorochrome-coupled antibodies (goat anti-rabbit conjugated to Alexa Fluor 488 [green] and goat anti-mouse conjugated to Alexa Fluor 594 [red], Life Technologies) were diluted 1:500. TO-PRO 3 (Life Technologies; 1:5000) was also used to mark the nucleus. Data were acquired with a

Fluoview 300 confocal microscope (Olympus, Center Valley, PA, USA).

Co-immunoprecipitation Assays. HEK293 cell lines stably expressing V5-tagged recombinant i1 and "empty" HEK293 cells were plated at a density of 5×10^6 cells per dish (100 mm) and transiently co-transfected 24 h later by electroporation with 20 μg of a pcDNA3 vector containing the untagged UGT2B7_v1, v2, or v4 cDNA sequences (encoding i1, i2, and i4 proteins, respectively). After 48 h, cells were lysed, and immunoprecipitation was performed with monoclonal anti-V5 (2 μg per ml of lysate) as described (Bellemare et al., 2010b), followed by SDS-PAGE of the samples and western blotting using anti-2B7 to detect the UGT2B7 variants (Millipore).

Analysis of Polysomes from HepG2 Cells. Cycloheximide at 100 μg/ml was added to the HepG2 cell medium and incubated 5 min at 37°C. HepG2 cells were then washed with ice-cold phosphate-buffered saline containing cycloheximide (100 μg/ml) and lysed in 200 μl of lysis buffer: 50 mM Tris-HCl pH 8.3, 150 mM KCl, 3 mM $MgCl_2$, 1% (w/v) IGEPAL, 10 mM dithiothreitol, 100 μg/ml cycloheximide, 200 μg/ml heparin, 100 U/ml Protector RNase Inhibitor (Roche Applied Science, Penzberg, Germany), and Complete protease inhibitor-EDTA-Free (Roche Applied Science). The addition of 10 mM EDTA into the lysis buffer of negative controls disrupted polysome aggregation and released translated mRNAs. Lysed cells were harvested with the use of a cell scraper. The complete protocol for polysome isolation has been described elsewhere (Scantland et al., 2011).

RESULTS

Heterologous Expression of UGT2B7 Truncated Proteins. We previously discovered two *UGT2B7* transcripts with a classical 5' region but alternative 3' ends, namely UGT2B7_v5 (containing a novel terminal exon 6b) and _v7 (exon 5 excluded) **(Fig. 1A).** The v1, v5 and v7 transcripts are co-expressed in human liver, kidney, and small intestine as well as in two human hepatic cell lines, HepG2 and C3A. HEK293 cells lack UGT expression and were initially used to overexpressed splice variant products (**Fig.1B**). Because we also wanted to study endogenous proteins, we selected two human cell lines expressing UGT2B7 splice variants v1, v5 and v7. These hepatic cell lines also exhibit glucuronidation activity for a selective substrate of UGT2B7 (AZT) (**Fig.1B**).

With the aim to assess protein expression in cellular models and human tissues, we initially tested three commercial UGT2B7 antibodies (Millipore, BD Gentest, and Abcam) on microsomes of HEK293 overexpressing UGT2Bs. Although the Millipore antibody was the most efficient at detecting the UGT2B7 enzyme (i1) and its cross-reaction with other UGT2Bs was minimal (**Fig. 2**), no immunoreactive signal was detected in human tissues at the molecular weights predicted for i2 and i4 isoforms, as assessed by western blotting (data not shown). The lack of a suitable antibody thus hindered detection of i2 and i4 in tissues or cell lines in which we observed v5 and v7 mRNAs. However, detection of full-length mRNAs in hepatocellular models such as HepG2 and its clonal derivative C3A (**Fig. 1B**) and the presence of alternate transcripts in isolated polysomes from these cells supported their endogenous translation to i2 and i4 proteins (**Fig. 3**). Also, variant UGT2B7 i2 and i4 proteins tagged with a V5 epitope were produced in HEK293 cells, an overexpression which was confirmed by western blotting using anti-V5 antibody (**Fig. 1D**).

Comparative Studies of Subcellular Localization of Variant UGT2B7 Proteins. Sequence analysis indicated that the predicted i2 and i4 proteins have a shorter C-terminal region, a feature that could impact subcellular localization (**Fig. 1C**). Cellular fractionation of clonal HEK293 cell lines expressing either i1 alone or with one variant (i2 or i4) demonstrated that all three UGT2B7 proteins co-localized in the microsomal/Golgi fraction (**Fig. 4A**). Moreover, a fraction of i2 and i4 could be recovered in the cytosolic fraction co-localizing with transketolase. The proper localization of subcellular compartment markers confirmed that the different organelles were correctly isolated in the three fractions (**Fig. 4B**). The localization of UGT2B7 variants in ER and Golgi was also confirmed in living cells by immunofluorescence experiments using calnexin and giantin as controls (**Fig. 5**).

UGT2B7 Truncated Isoforms Suppress AZT Glucuronidation Activity Likely through Direct Protein-protein Interaction. We previously showed that the UGT2B7_i2 and i4 proteins are enzymatically inactive on classical UGT2B7 substrates (Menard et al., 2011). However, in UGT2B7-overexpressing HEK293 cell lines the presence of i2 or i4 significantly decreased the extent of i1-mediated AZT-G formation by up to 40% compared with cells expressing only i1 **(Fig. 6A).** There was no significant difference in K_m values among the clonal cell lines, and all data were consistent with Michaelis-Menten kinetics (**Supplemental Figure 1**). At the K_m (1550 μM), AZT-G formation was reduced by 41% in the presence of i2 and by 48% with i4. At a fixed substrate concentration (200 μM AZT) and variable concentrations of co-substrate UDP-glucuronic acid (50–5000 μM), i2 or i4 caused an 80% decrease in Vmax with no change in K_m (data not shown). As protein-protein interactions are a potential mechanism underlying the

inhibitory effect of i2 and i4 on UGT2B7 activity, we examined if i2 and i4 interact with i1. Co-immunoprecipitation experiments were performed using HEK293 cell lines expressing i1-tagV5 + i2 (**Fig. 6B**) or i1-tagV5 + i4 (**Fig. 6C**). We observed that the untagged i2 and i4 co-immunoprecipitated with i1-tagV5. Because of an apparent weaker i1-i4 interaction (likely caused by inferior transient expression of v7 in HEK293 cells), this observation was confirmed using hemagglutinin (HA)-tagged i1 and V5-tagged i4 overexpressed proteins and a hemagglutinin column in a co-IP experiment (data not shown).

Overexpression or Repression of UGT2B7 Splice Variants Modifies UGT2B7-mediated Activity in Hepatic Cells. The effect of ectopic expression of i2 or i4 (with or without a C-terminal V5 tag) was further assessed using HepG2 cells as a model—this cell line endogenously expresses enzymatically active UGT2B7_i1 and its splice variants (**Fig. 1B**). Following overexpression of i2 or i4, AZT-G formation decreased significantly by at least 20% regardless of the presence of the tag (**Fig. 7**). Notably, overexpression of splice variants was confirmed by the detection of ex5-ex6b and ex4-ex6a alternative splicing events by qPCR; representing less that 10% of the expression of v1 transcripts. By using specific siRNA-mediated knockdown, we then evaluated whether repression of splice variants could influence UGT2B7 activity: we initially tested the hepatoma-derived HepG2 cells and further confirmed the effect in the clonal cell line C3A, both of which express v1, v5, and v7 mRNAs endogenously (**Fig. 1B**). **Figure 8** illustrates that partial repression by 70% and 62% of v5 mRNA levels in HepG2 and C3A cells increased AZT-G formation (ranging from 20 to 72%). In addition, repression of v7 mRNA (by 54%) increased UGT2B7 activity by 110% in C3A cells. All observed changes were statistically significant except for the v7 knockdown in HepG2 cells, in which the ex4-ex6a siRNA had a

relatively weak effect on v7 mRNA expression and AZT glucuronidation activity. In all conditions, the levels of v1 expression were unaffected. Additional glucuronidation assays also showed no significant changes in the formation of estradiol-3G, a reaction catalyzed by few UGT1As including UGT1A1 (results not shown).

DISCUSSION

We report that co-overexpression of the enzymatically active UGT2B7_i1 with i2 or i4 splice forms in HEK293 (UGT negative) cells and in HepG2 cells (which endogenously express i1, i2, and i4) led to a significant reduction of UGT2B7-mediated glucuronidation. On the other hand, siRNA-mediated partial depletion of endogenous variant UGT2B7 transcripts v5 and v7 led to increased cellular glucuronidation. We were able to detect the expression of the novel v5 and v7 transcripts in human liver, kidney, and small intestine as well as in liver cell lines, but the absence of a specific antibody for i2 and i4 prohibited detection of these proteins. However, the full-length v5 and v7 transcripts could be detected in translated mRNAs found in polyribosomal fractions of HepG2 and C3A cells, confirming the production of i2 and i4 proteins in those cell lines. Also, overexpression of v5 and v7 in HEK293 cells gave rise to detectable i2 and i4 proteins in Golgi and ER, which hints further toward the functional translatability of these variants in cells. The enzyme kinetics for AZT, a probe substrate for UGT2B7, showed that the apparent affinity (K_m) was not affected by i2 and i4 whereas the V_{max} was significantly reduced compared with cells expressing only the i1 enzyme. The lowering of the V_{max} of UGT2B7_i1 by i2 and i4 suggests that the inhibitory mechanism of the alternative isoforms could be through a decrease in the concentration of active UGT2B7 enzymes; in support of this idea, we further demonstrated the potential of each of the two UGT2B7 C-terminally truncated proteins to interact with the i1 enzyme. This mechanism likely results in the trapping of the active UGT2B7 enzyme in an inactive higher-order complex, thus hindering glucuronidation. These observations are in line with our previous reports of the regulatory influence of enzymatically inactive truncated isoforms 2 derived from the inclusion of an alternative exon 5 (5b) at the *UGT1A* locus on cellular glucuronidation (Bellemare et al., 2010b; Bellemare et al., 2010c).

Regarding protein-protein interactions, the homodimerization of UGT2B7 has been reported (Lewis et al., 2011), a feature also observed herein (data not shown). Our data are in line with previous reports of the oligomerization of UGT2B7 with other UGTs and CYPs, a process that appears to modulate glucuronidation rates (Fremont et al., 2005; Takeda et al., 2005; Takeda et al., 2009; Fujiwara et al., 2010). Furthermore, UGT2B7 dimerization was identified as a possible causal factor for the atypical sigmoidal kinetics of glucuronidation by UGT2B7 of 4-methylumbelliferone and 1-naphtol, these kinetics fitting well with a "two-site" model in which two distinct substrate-binding sites coexist (Uchaipichat et al., 2008). The replacement of a putative "dimerization signature motif" ($_{183}$HSGGFIFPPSYVPVVMS$_{200}$E) in UGT2B7 by a UGT2B15 homologous peptide sequence led to the loss of atypical kinetics of glucuronidation of 4-methylumbelliferone (Lewis et al., 2007), a feature attributable to unsuccessful homodimerization of the enzyme (Lewis et al., 2011). Interestingly, this potential dimerization motif is present in UGT2B7 i2 and i4 and thus could allow interaction with the UGT2B7 enzyme, as we observed. Full-length alternative transcripts are co-expressed with the UGT2B7 enzyme in human liver, kidney, and small intestine, and all three UGT2B7 expressed proteins are found in the same subcellular compartments, thus suggesting that these interactions might occur *in vivo*. However, UGT2B7 splice variants were determined to have no effect on the glucuronidation activity of estradiol at position 3 that is performed by UGT1As namely UGT1A1, suggesting that their modulatory effects could be specific to UGT2B7 enzyme. This observation is consistent with a previous study showing that coexpression of UGT2A1_i1 or UGT2A1_i2 with other UGT1A or UGT2B enzymes caused no change in UGT1A or UGT2B glucuronidation activity (Bushey and Lazarus, 2012). Additional investigations are needed to better understand the

oligomerization of UGT2B7 with its alternative splicing partners as well as with other UGT pathways and its impact on glucuronidation activity *in vivo*.

Because i2 and i4 lack the transmembrane domain $_{493}$VIGFLLVCVATVIFIV$_{509}$ (Mackenzie, 1986; Radominska-Pandya et al., 2010), their presence in Golgi and ER membranes and not exclusively in the cytosol observed by immunofluorescence could seem unexpected; however, C-terminal variants of UGT2B4 and UGT1A also lacking this conserved domain were found to be ER membrane-bound (Levesque et al., 2007; Levesque et al., 2010). An explanation for membrane retention of a fraction of the total amount of i4 could reside in the presence of two positively charged residues, lysine and arginine, near its alternative C-terminal end ($_{364}$DI**K**$^{+}$**R**$^{+}$M$_{369}$L), a feature very similar to the retention of UGT1A_i2s as a consequence of its C-terminal dilysine motif (Levesque et al., 2007). Moreover, three of the other four amino acids are hydrophobic (isoleucine, methionine, leucine), also potentially favoring membrane retention (Rosch et al., 2000). The terminal sequence of i2 comprises a stretch of seven hydrophobic residues and one positively charged lysine out of 12 residues ($_{444}$IAASCGNCMFMK$_{456}$), a sequence that could participate in the retention of the variant polypeptide in the ER. We also report the presence of i1, i2, and i4 in the Golgi, a feature that is compatible with scarce reports of weak UGT activity in this organelle (von Bahr et al., 1972; Bossuyt and Blanckaert, 2001). However, it is also plausible that these three proteins undergo chemical modifications in the Golgi; indeed, UGT2B7 is glycosylated (Nagaoka et al., 2012), a chemical modification mainly initiated and/or terminated in the Golgi (Stanley, 2011). Western blotting of centrifugation fractions and comparison of UGT2B7 signals with subcellular compartment–specific markers further substantiates that i1, i2, and i4 are all residents of the ER and Golgi, whereas i2 and i4 can

also be found in the cytoplasm, where they may have roles distinct from that of i1 inhibition. On the other hand, this observation could also mean that a fraction of the pool of UGT2B7 truncated proteins is recognized by the ER ultra-specialized machinery as being misfolded and thus sent back to the cytosol to be degraded by the proteasome (Petris et al., 2011). The consensus is that misfolded and/or deleterious polypeptides are recognized at one of various checkpoints by the proteins of the ERAD ("endoplasmic reticulum–associated degradation") pathway and are retrotranslocated and proteolyzed before their migration to the *cis* region of the Golgi (Ellgaard and Helenius, 2003). Thus, the apparent localization of i2 and i4 in both the ER and Golgi along with the UGT2B7 enzyme suggests that these isoforms fold correctly and thus generally are not subjected to degradation, which is also substantiated by the observed alteration of the glucuronidation phenotype upon their overexpression or partial depletion.

Levels of endogenous i2 and i4 relative to the i1 protein could not be measured. However, we observed that the coexpression of the UGT2B7 enzyme in HEK293 with inferior levels of the i2 or i4 proteins (35% and 10% of i1, respectively) yielded a significant repression of AZT-G formation. In hepatic cell lines (HepG2 and C3A), the relative expression of v5 and v7 mRNAs was less than 10% that of v1 transcripts encoding the UGT2B7 enzyme with significant changes in UGT2B7-mediated activity (up to 72% increased AZT-G formation) upon partial depletion of endogenous v5 and v7 variants. Data suggest that high levels of splice forms might not be required to have a meaningful impact on cellular glucuronidation. The mRNA levels of UGT2B7 splice forms observed in hepatic cell lines are similar to what was reported recently for v2/v3 splice variants encoding UGT1A_i2s in human liver samples (Jones et al., 2012). Also, Court and collaborators suggest that UGT1A-3′UTR SNPs associated with a decreased risk of

unintentional acetaminophen-induced acute liver failure might regulate exon 5a/5b splicing in the liver (Court et al., 2013). One could speculate that changes in UGT splicing ratios, even when splicing forms are not abundant relative to transcripts producing UGT enzymes, may have important phenotypic effects.

Our conclusion is that a potential novel auto-regulatory mechanism of the UGT2B7 glucuronidation pathway is mediated by the alternative proteins.

ACKNOWLEDGMENTS

The authors thank Patrick Caron for mass spectrometry–based assays for glucuronide detection as well as Olivier Eap, Mario Harvey, and Lyne Villeneuve for technical support.

AUTHORSHIP CONTRIBUTION

Participated in research design: Guillemette

Conducted experiments: Ménard, Collin, Margaillan

Performed data analysis: Ménard, Guillemette

Wrote or contributed to the writing of the manuscript: Ménard, Collin, Margaillan, Guillemette

REFERENCES

Barbier O, Turgeon D, Girard C, Green MD, Tephly TR, Hum DW, and Belanger A (2000) 3'-azido-3'-deoxythimidine (AZT) is glucuronidated by human UDP-glucuronosyltransferase 2B7 (UGT2B7). *Drug metabolism and disposition: the biological fate of chemicals* **28:**497-502.

Belanger AS, Caron P, Harvey M, Zimmerman PA, Mehlotra RK, and Guillemette C (2009) Glucuronidation of the antiretroviral drug efavirenz by UGT2B7 and an in vitro investigation of drug-drug interaction with zidovudine. *Drug metabolism and disposition: the biological fate of chemicals* **37:**1793-1796.

Bellemare J, Rouleau M, Girard H, Harvey M, and Guillemette C (2010a) Alternatively spliced products of the UGT1A gene interact with the enzymatically active proteins to inhibit glucuronosyltransferase activity in vitro. *Drug metabolism and disposition: the biological fate of chemicals* **38:**1785-1789.

Bellemare J, Rouleau M, Harvey M, and Guillemette C (2010b) Modulation of the human glucuronosyltransferase UGT1A pathway by splice isoform polypeptides is mediated through protein-protein interactions. *The Journal of biological chemistry* **285:**3600-3607.

Bellemare J, Rouleau M, Harvey M, Tetu B, and Guillemette C (2010c) Alternative-splicing forms of the major phase II conjugating UGT1A gene negatively regulate glucuronidation in human carcinoma cell lines. *The pharmacogenomics journal* **10:**431-441.

Bossuyt X and Blanckaert N (2001) Differential regulation of UDP-GlcUA transport in endoplasmic reticulum and in Golgi membranes. *Journal of hepatology* **34:**210-214.

Bushey RT and Lazarus P (2012) Identification and functional characterization of a novel UDP-glucuronosyltransferase 2A1 splice variant: potential importance in tobacco-related cancer susceptibility. *The Journal of pharmacology and experimental therapeutics* **343:**712-724.

Court MH, Freytsis M, Wang X, Peter I, Guillemette C, Hazarika S, Duan SX, Greenblatt DJ, and Lee WM (2013) The UDP-glucuronosyltransferase (UGT) 1A polymorphism c.2042C>G (rs8330) is associated with increased human liver acetaminophen glucuronidation, increased UGT1A exon 5a/5b splice variant mRNA ratio, and decreased risk of unintentional acetaminophen-induced acute liver failure. *The Journal of pharmacology and experimental therapeutics* **345:**297-307.

Court MH, Zhang X, Ding X, Yee KK, Hesse LM, and Finel M (2012) Quantitative distribution of mRNAs encoding the 19 human UDP-glucuronosyltransferase enzymes in 26 adult and 3 fetal tissues. *Xenobiotica; the fate of foreign compounds in biological systems* **42:**266-277.

Ellgaard L and Helenius A (2003) Quality control in the endoplasmic reticulum. *Nature reviews Molecular cell biology* **4:**181-191.

Filippi C, Keatch SA, Rangar D, Nelson LJ, Hayes PC, and Plevris JN (2004) Improvement of C3A cell metabolism for usage in bioartificial liver support systems. *Journal of hepatology* **41:**599-605.

Fremont JJ, Wang RW, and King CD (2005) Coimmunoprecipitation of UDP-glucuronosyltransferase isoforms and cytochrome P450 3A4. *Molecular pharmacology* **67:**260-262.

Fujiwara R, Nakajima M, Oda S, Yamanaka H, Ikushiro S, Sakaki T, and Yokoi T (2010) Interactions between human UDP-glucuronosyltransferase (UGT) 2B7 and UGT1A enzymes. *Journal of pharmaceutical sciences* **99:**442-454.

Girard H, Levesque E, Bellemare J, Journault K, Caillier B, and Guillemette C (2007) Genetic diversity at the UGT1 locus is amplified by a novel 3' alternative splicing mechanism leading to nine additional UGT1A proteins that act as regulators of glucuronidation activity. *Pharmacogenetics and genomics* **17:**1077-1089.

Guillemette C, Levesque E, Beaulieu M, Turgeon D, Hum DW, and Belanger A (1997) Differential regulation of two uridine diphospho-glucuronosyltransferases, UGT2B15 and UGT2B17, in human prostate LNCaP cells. *Endocrinology* **138:**2998-3005.

Guillemette C, Levesque E, Harvey M, Bellemare J, and Menard V (2010) UGT genomic diversity: beyond gene duplication. *Drug metabolism reviews* **42:**24-44.

He D, Frost AR, and Falany CN (2005) Identification and immunohistochemical localization of Sulfotransferase 2B1b (SULT2B1b) in human lung. *Biochimica et biophysica acta* **1724:**119-126.

Innocenti F, Liu W, Fackenthal D, Ramirez J, Chen P, Ye X, Wu X, Zhang W, Mirkov S, Das S, Cook E, Jr., and Ratain MJ (2008) Single nucleotide polymorphism discovery and functional assessment of variation in the UDP-glucuronosyltransferase 2B7 gene. *Pharmacogenetics and genomics* **18:**683-697.

Jin CJ, Mackenzie PI, and Miners JO (1997) The regio- and stereo-selectivity of C19 and C21 hydroxysteroid glucuronidation by UGT2B7 and UGT2B11. *Archives of biochemistry and biophysics* **341:**207-211.

Jones NR, Sun D, Freeman WM, and Lazarus P (2012) Quantification of Hepatic UDP glucuronosyltransferase 1A splice variant expression and correlation of UDP glucuronosyltransferase 1A1 variant expression with glucuronidation activity. *The Journal of pharmacology and experimental therapeutics* **342:**720-729.

Lepine J, Bernard O, Plante M, Tetu B, Pelletier G, Labrie F, Belanger A, and Guillemette C (2004) Specificity and regioselectivity of the conjugation of estradiol, estrone, and their catecholestrogen and methoxyestrogen metabolites by human uridine diphospho-glucuronosyltransferases expressed in endometrium. *The Journal of clinical endocrinology and metabolism* **89:**5222-5232.

Levesque E, Girard H, Journault K, Lepine J, and Guillemette C (2007) Regulation of the UGT1A1 bilirubin-conjugating pathway: role of a new splicing event at the UGT1A locus. *Hepatology* **45:**128-138.

Levesque E, Menard V, Laverdiere I, Bellemare J, Barbier O, Girard H, and Guillemette C (2010) Extensive splicing of transcripts encoding the bile acid-conjugating enzyme UGT2B4 modulates glucuronidation. *Pharmacogenetics and genomics* **20:**195-210.

Lewis BC, Mackenzie PI, Elliot DJ, Burchell B, Bhasker CR, and Miners JO (2007) Amino terminal domains of human UDP-glucuronosyltransferases (UGT) 2B7 and 2B15 associated with substrate selectivity and autoactivation. *Biochemical pharmacology* **73:**1463-1473.

Lewis BC, Mackenzie PI, and Miners JO (2011) Homodimerization of UDP-glucuronosyltransferase 2B7 (UGT2B7) and identification of a putative dimerization domain by protein homology modeling. *Biochemical pharmacology* **82:**2016-2023.

Mackenzie PI (1986) Rat liver UDP-glucuronosyltransferase. Sequence and expression of a cDNA encoding a phenobarbital-inducible form. *The Journal of biological chemistry* **261:**6119-6125.

Mackenzie PI, Bock KW, Burchell B, Guillemette C, Ikushiro S, Iyanagi T, Miners JO, Owens IS, and Nebert DW (2005) Nomenclature update for the mammalian UDP glycosyltransferase (UGT) gene superfamily. *Pharmacogenetics and genomics* **15:**677-685.

Mano Y, Usui T, and Kamimura H (2007) The UDP-glucuronosyltransferase 2B7 isozyme is responsible for gemfibrozil glucuronidation in the human liver. *Drug metabolism and disposition: the biological fate of chemicals* **35:**2040-2044.

Menard V, Eap O, Roberge J, Harvey M, Levesque E, and Guillemette C (2011) Transcriptional diversity at the UGT2B7 locus is dictated by extensive pre-mRNA splicing mechanisms that give rise to multiple mRNA splice variants. *Pharmacogenetics and genomics* **21:**631-641.

Nagaoka K, Hanioka N, Ikushiro S, Yamano S, and Narimatsu S (2012) The effects of N-glycosylation on the glucuronidation of zidovudine and morphine by UGT2B7 expressed in HEK293 cells. *Drug metabolism and pharmacokinetics*.

Nakamura A, Nakajima M, Yamanaka H, Fujiwara R, and Yokoi T (2008) Expression of UGT1A and UGT2B mRNA in human normal tissues and various cell lines. *Drug metabolism and disposition: the biological fate of chemicals* **36:**1461-1464.

Pan Q, Shai O, Lee LJ, Frey BJ, and Blencowe BJ (2008) Deep surveying of alternative splicing complexity in the human transcriptome by high-throughput sequencing. *Nature genetics* **40:**1413-1415.

Petris G, Vecchi L, Bestagno M, and Burrone OR (2011) Efficient detection of proteins retro-translocated from the ER to the cytosol by in vivo biotinylation. *PloS one* **6:**e23712.

Radominska-Pandya A, Bratton SM, Redinbo MR, and Miley MJ (2010) The crystal structure of human UDP-glucuronosyltransferase 2B7 C-terminal end is the first mammalian UGT target to be revealed: the significance for human UGTs from both the 1A and 2B families. *Drug metabolism reviews* **42:**133-144.

Rosch K, Naeher D, Laird V, Goder V, and Spiess M (2000) The topogenic contribution of uncharged amino acids on signal sequence orientation in the endoplasmic reticulum. *The Journal of biological chemistry* **275:**14916-14922.

Ross VL and Board PG (1993) Molecular cloning and heterologous expression of an alternatively spliced human Mu class glutathione S-transferase transcript. *The Biochemical journal* **294 (Pt 2):**373-380.

Scantland S, Grenon JP, Desrochers MH, Sirard MA, Khandjian EW, and Robert C (2011) Method to isolate polyribosomal mRNA from scarce samples such as mammalian oocytes and early embryos. *BMC developmental biology* **11:**8.

Stanley P (2011) Golgi glycosylation. *Cold Spring Harbor perspectives in biology* **3**.

Stone AN, Mackenzie PI, Galetin A, Houston JB, and Miners JO (2003) Isoform selectivity and kinetics of morphine 3- and 6-glucuronidation by human udp-glucuronosyltransferases: evidence for atypical glucuronidation kinetics by UGT2B7. *Drug metabolism and disposition: the biological fate of chemicals* **31:**1086-1089.

Takeda S, Ishii Y, Iwanaga M, Nurrochmad A, Ito Y, Mackenzie PI, Nagata K, Yamazoe Y, Oguri K, and Yamada H (2009) Interaction of cytochrome P450 3A4 and UDP-

glucuronosyltransferase 2B7: evidence for protein-protein association and possible involvement of CYP3A4 J-helix in the interaction. *Molecular pharmacology* **75:**956-964.

Takeda S, Ishii Y, Mackenzie PI, Nagata K, Yamazoe Y, Oguri K, and Yamada H (2005) Modulation of UDP-glucuronosyltransferase 2B7 function by cytochrome P450s in vitro: differential effects of CYP1A2, CYP2C9 and CYP3A4. *Biological & pharmaceutical bulletin* **28:**2026-2027.

Thibaudeau J, Lepine J, Tojcic J, Duguay Y, Pelletier G, Plante M, Brisson J, Tetu B, Jacob S, Perusse L, Belanger A, and Guillemette C (2006) Characterization of common UGT1A8, UGT1A9, and UGT2B7 variants with different capacities to inactivate mutagenic 4-hydroxylated metabolites of estradiol and estrone. *Cancer research* **66:**125-133.

Tojcic J, Benoit-Biancamano MO, Court MH, Straka RJ, Caron P, and Guillemette C (2009) In vitro glucuronidation of fenofibric acid by human UDP-glucuronosyltransferases and liver microsomes. *Drug metabolism and disposition: the biological fate of chemicals* **37:**2236-2243.

Trottier J, Perreault M, Rudkowska I, Levy C, Dallaire-Theroux A, Verreault M, Caron P, Staels B, Vohl MC, Straka RJ, and Barbier O (2013) Profiling serum bile acid glucuronides in humans: gender divergences, genetic determinants and response to fenofibrate. *Clinical pharmacology and therapeutics*.

Turgeon D, Chouinard S, Belanger P, Picard S, Labbe JF, Borgeat P, and Belanger A (2003) Glucuronidation of arachidonic and linoleic acid metabolites by human UDP-glucuronosyltransferases. *Journal of lipid research* **44:**1182-1191.

Turman CM, Hatley JM, Ryder DJ, Ravindranath V, and Strobel HW (2006) Alternative splicing within the human cytochrome P450 superfamily with an emphasis on the brain: The convolution continues. *Expert opinion on drug metabolism & toxicology* **2:**399-418.

Uchaipichat V, Galetin A, Houston JB, Mackenzie PI, Williams JA, and Miners JO (2008) Kinetic modeling of the interactions between 4-methylumbelliferone, 1-naphthol, and zidovudine glucuronidation by udp-glucuronosyltransferase 2B7 (UGT2B7) provides evidence for multiple substrate binding and effector sites. *Molecular pharmacology* **74:**1152-1162.

von Bahr C, Hietanen E, and Glaumann H (1972) Oxidation and glucuronidation of certain drugs in various subcellular fractions of rat liver: binding of desmethylimipramine and hexobarbital to cytochrome P-450 and oxidation and glucuronidation of desmethylimipramine, aminopyrine, p-nitrophenol and 1-naphthol. *Acta pharmacologica et toxicologica* **31:**107-120.

FOOTNOTES

This work was supported by the Canadian Institutes of Health Research (CIHR) [MOP-42392]. V.M. was a recipient of a CIHR Frederick Banting and Charles Best studentship award. G.M. is recipient of a studentship award from *'Fonds de l'enseignement et de la recherche'* of the Faculty of pharmacy, Laval University. P.C. was a recipient of a "*Fonds de recherches en santé du Québec*" studentship award. C.G. holds the Canada Research Chair in Pharmacogenomics.

Disclosures: The authors have no conflicts of interests to disclose.

FIGURE LEGENDS

Figure 1 – UGT2B7 splice variants. A) mRNA structure of two alternative transcripts (named v5 and v7) and the canonical v1 derived from human *UGT2B7* by alternative splicing. **B)** RT-PCR amplification of v1, v5, and v7 in total RNA from human liver (L), kidney (K) and small intestine (SI) from three individuals as well as selected cell lines (HepG2, C3A, and HEK293). **C)** Peptide sequence representation of variant isoforms (i1, i2, and i4) derived respectively from v1, v5, and v7 transcripts. Protein domains are also indicated. aa: amino acids. **D)** Overexpression of UGT2B7 variants in HEK293 cells (UGT2B7-negative). Clones overexpressing each individual protein (i1, i2, or i4) or double-transfectants (i1+i2 and i1+i4) were produced, and protein expression was confirmed using an anti-V5 antibody. The UGT2B7-overexpressing cell lines displayed a 1:0.35 (i1:i2) and 1:0.1 (i1:i4) ratios.

Figure 2 – Specificity of commercial antibodies against UGT2B7 and other UGT2B family members. To test the specificity of commercial antibodies against UGT2B7, we used 20 µg of microsomes derived from clonal HEK293 cells stably expressing UGT2B isoforms in 10% SDS-PAGE experiments. Antibodies were used as suggested by the manufacturers (Millipore, Gentest, and Abcam), and results were compared with experiments using an anti-UGT2B antibody (EL-93 targeting the C-terminal extremity of UGT2B proteins). An arrow identifies UGT2B7 signals. NS, non-specific marking of the antibody.

Figure 3 – Isolation of polysomal fractions from liver cells supporting translation of UGT2B7 mRNA variants v1, v5, and v7. *Upper panel: Fractionation of cytosolic extracts from HepG2 cells through a linear sucrose gradient (15–45%).* The chromatogram illustrates the separation of HepG2 cytosolic extracts at assessed by measuring absorbance (254 nm) in the

absence (filled line) or presence (dashed line) of EDTA. A similar pattern was observed with C3A cells (not shown). The polysomes were found in fractions 6–11 (–EDTA), whereas monosomes were mainly found in earlier fractions. The presence of EDTA breaks polysomes into ribosomal subunits leading to the release of translated mRNAs (+EDTA). *Lower panel: Detection of UGT2B7 mRNA variants in polysomal fractions by specific PCR amplification.* For each fraction, we assessed the presence of three UGT2B7 mRNA variants, namely UGT2B7_v1 (positive control), v5, and v7. As expected for translated mRNA, specific PCR products were mostly observed in polysomal fractions in the absence of EDTA. In contrast, the presence of EDTA shifted specific PCR products toward monosomes (80S) and ribosomal subunits (40S and 60S).

Figure 4 – Cellular localization of UGT2B7 protein variants. Cellular fractions (microsomes/Golgi (M+G), whole cells/nuclei (W+N), and cytosol (C)) from HEK293 cells overexpressing i1, i1+i2, or i1+i4 were separated by 10% SDS-PAGE. Proteins were detected with rabbit polyclonal anti-UGT2B7 (Millipore, 1:1000) (**A**, top panel) and monoclonal anti-V5 tag (1:5000) (**A**, bottom panel). As positive controls to mark specific subcellular structures, we used anti-calnexin for the ER (**B**, top panel), anti-RCAS1 for the Golgi (**B**, middle panel), and anti-transketolase for the cytoplasm (**B**, bottom panel). Arrows indicate detected proteins.

Figure 5 – Cellular localization by immunofluorescence. The subcellular localization of UGT2B7 proteins (V5-tagged proteins) was superimposed with the staining of calnexin, an ER resident protein (**A**), and giantin, a maker for the Golgi (**B**). HEK293 cells were used as a negative control.

Figure 6 – Kinetics of AZT glucuronidation assessed in HEK293 cells overexpressing UGT2B7 splice variants and co-immunoprecipitation assays supporting a protein-protein interaction between i1 and truncated variants i2 and i4. (A) Rates of formation of AZT-G for HEK293 cell lines. Variant proteins were tagged with a V5 epitope; similar results were observed with untagged UGT2B7 variants (data not shown). Kinetic parameters (V_{max} and Km) are shown below the graph and were fitted to a Michaelis-Menten profile consistent with previous reports (Barbier et al., 2000) (**Supplemental Figure 1** displays Eadie-Hofstee plots). All data represent the mean ± SD of two independent experiments performed in triplicate and normalized for UGT2B7 enzyme expression (i1), *P<0.05. **(B and C)** Co-immunoprecipitation experiments support the interaction between the active i1 UGT2B7 enzyme and splice variants i2 (**B**) and i4 (**C**). The i1 protein was V5-tagged, whereas UGT2B7 variants were not tagged for transient expression. In all cases, monoclonal anti-V5 was used for immunoprecipitation (IP), whereas polyclonal anti-UGT2B7 (Millipore) was used to visualize the resulting bands in 10% SDS-PAGE migration experiments. Lanes 1, 2 and 3: IP with anti-V5 (1 µg). Lane 1, i1-V5 + untagged isoform (i1, i2 or i4); lane 2, untagged isoform (i1, i2 or i4), negative control; lane 3, i1-V5, positive control for i1-V5 expression. Lane 4, IP with rabbit Ig-G (1 µg), i1-V5 + untagged isoform (i1, i2 or i4), control for the specificity of IP.

Figure 7 – Overexpression of i2 and i4 proteins in HepG2 cells impacts the rate of AZT-G formation. Microsomal extracts (20 µg) from i2- or i4-overexpressing HepG2 cell lines were used to assess UGT2B7-mediated AZT glucuronidation (top panel) and compared with the glucuronidation activity of a pcDNA6-overexpressing HepG2 cells. Data are given as the mean ± S.D. of at least of two independent experiments performed in triplicate and normalized for

UGT2B7 enzyme expression (i1), *P<0.05. Quantification of a characteristic splicing event for each transgene by qPCR is expressed as the number of copies per 10,000 copies of RPLP0 (36B4, control gene) (middle panel). The bottom panel depicts a graphical representation of the real-time PCR amplification strategies used to delineate the occurrence of ex5-ex6a, ex5-ex6b, and ex4-ex6a; those splicing events were mainly noted in v1, v5, and v7 transcripts, respectively.

Figure 8 – Knockdown of endogenous UGT2B7 alternative transcripts by RNA interference induces glucuronidation activity of two human liver cell lines. A) Schematic representation of the *UGT2B7* region targeted by each siRNA. UTR: untranslated region. **B)** Changes in expression were evaluated by qPCR and reported as relative expression to a non-target siRNA control; *P<0.05. **C)** Glucuronidation assays were performed with cell homogenates (50 µg) incubated 4 h with 200 µM AZT. Data are displayed as the mean ± S.D. of two independent experiments performed in triplicate and normalized for UGT2B7 enzyme expression (i1); *P<0.05.

Figure 1

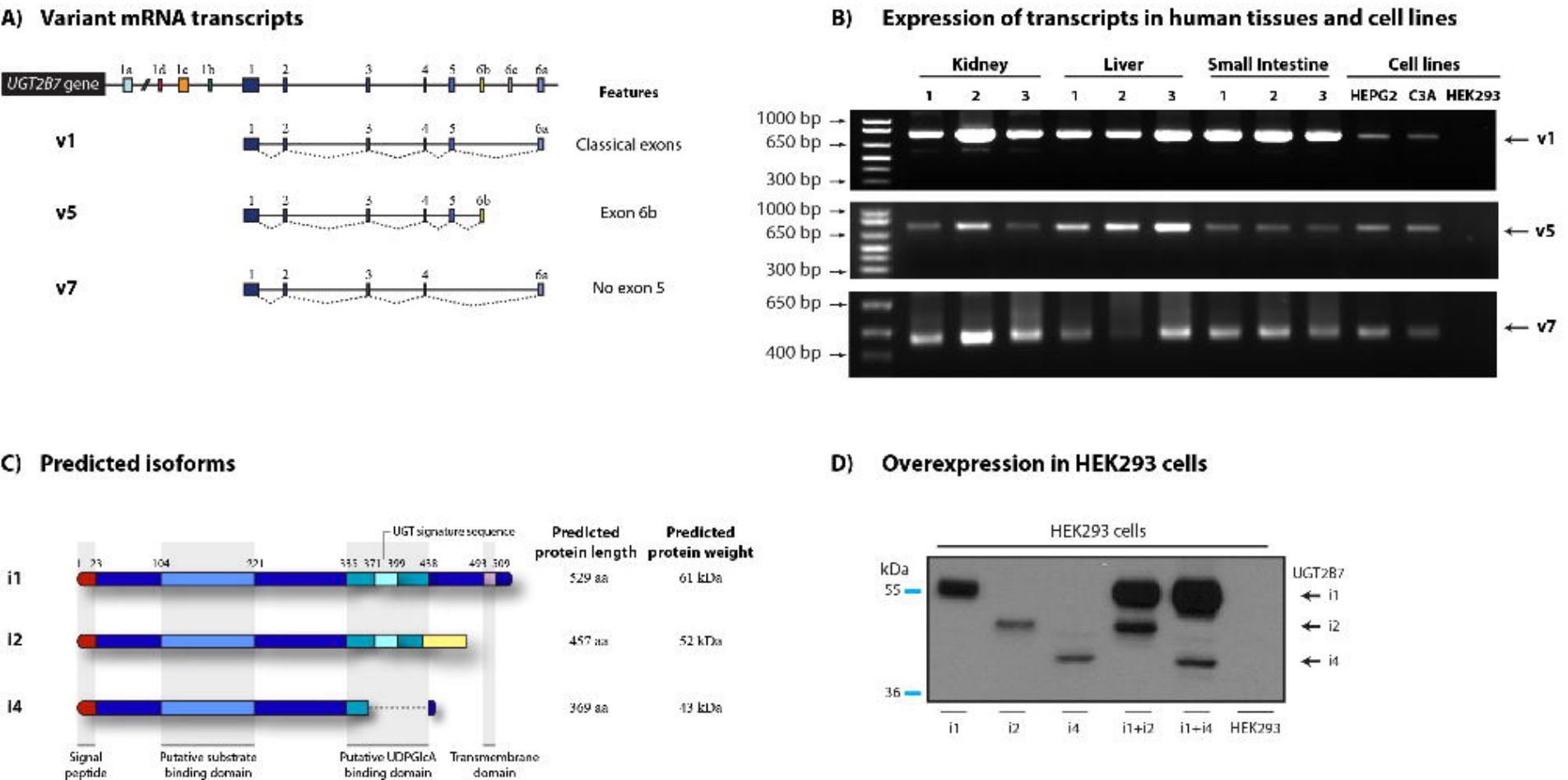
A) Variant mRNA transcripts
UGT2B7 gene
Features
v1
Classical exons
v5
Exon 6b
v7
No exon 5
B) Expression of transcripts in human tissues and cell lines
Kidney
Liver
Small Intestine
Cell lines
HEPG2
C3A
HEK293
1000 bp
650 bp
300 bp
400 bp
C) Predicted isoforms
UGT signature sequence
Predicted protein length
Predicted protein weight
i1
529 aa
61 kDa
i2
457 aa
52 kDa
i4
369 aa
43 kDa
Signal peptide
Putative substrate binding domain
Putative UDPGlcA binding domain
Transmembrane domain
D) Overexpression in HEK293 cells
HEK293 cells
kDa
55
36
UGT2B7
i1
i2
i4
i1+i2
i1+i4
HEK293

Figure 2

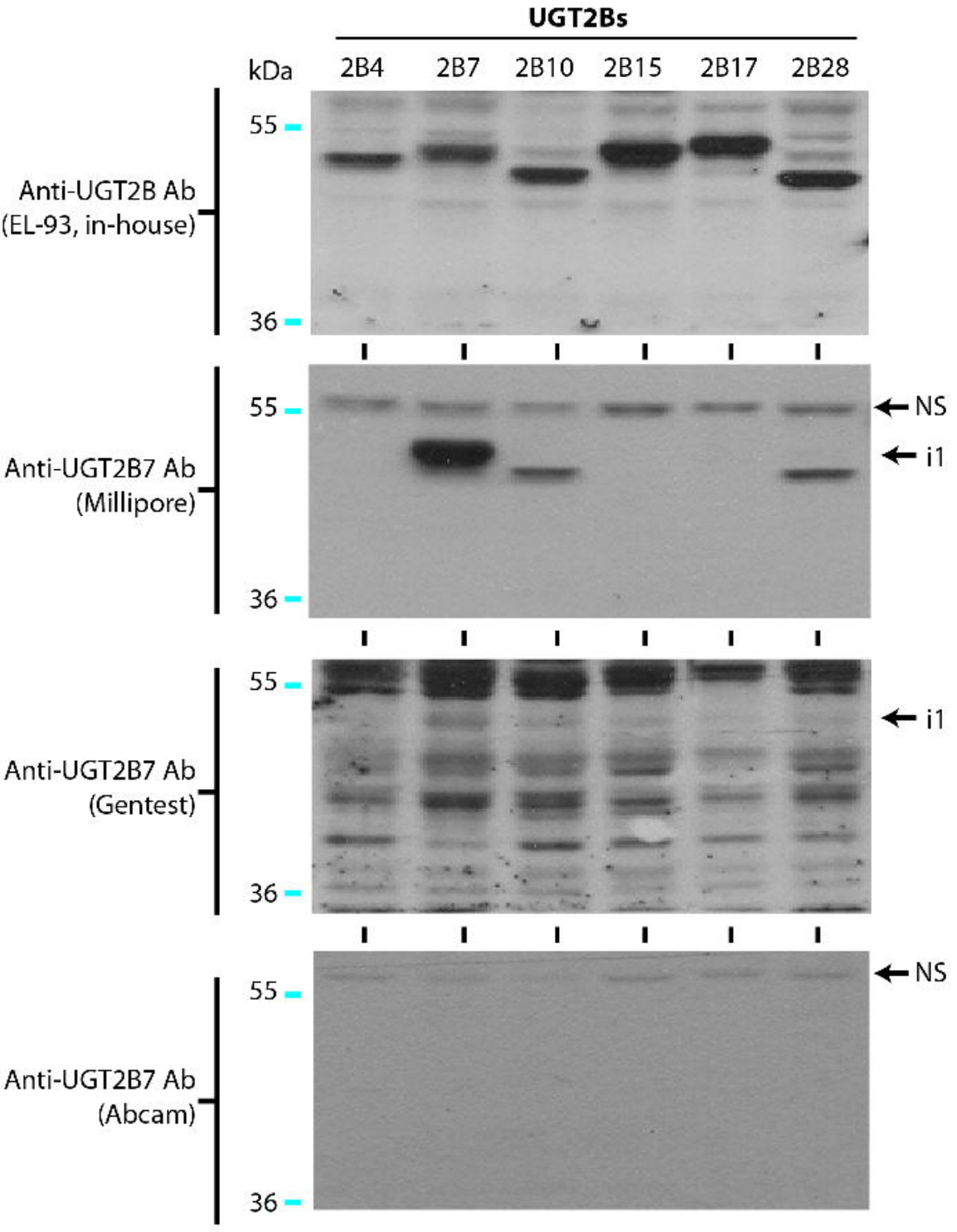

NS = Non-specific marking

Figure 3

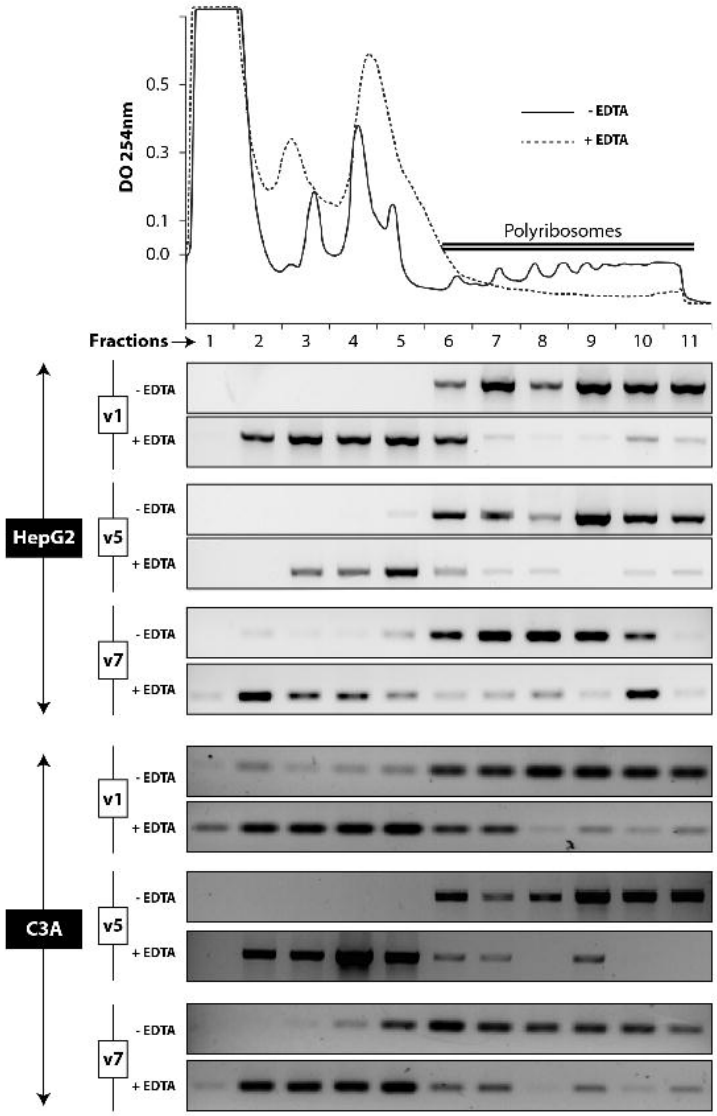
DO 254nm
0.5
0.3
0.1
0.0
- EDTA
+ EDTA
Polyribosomes
Fractions → 1 2 3 4 5 6 7 8 9 10 11
HepG2
C3A
v1
v5
v7
- EDTA
+ EDTA

Figure 4

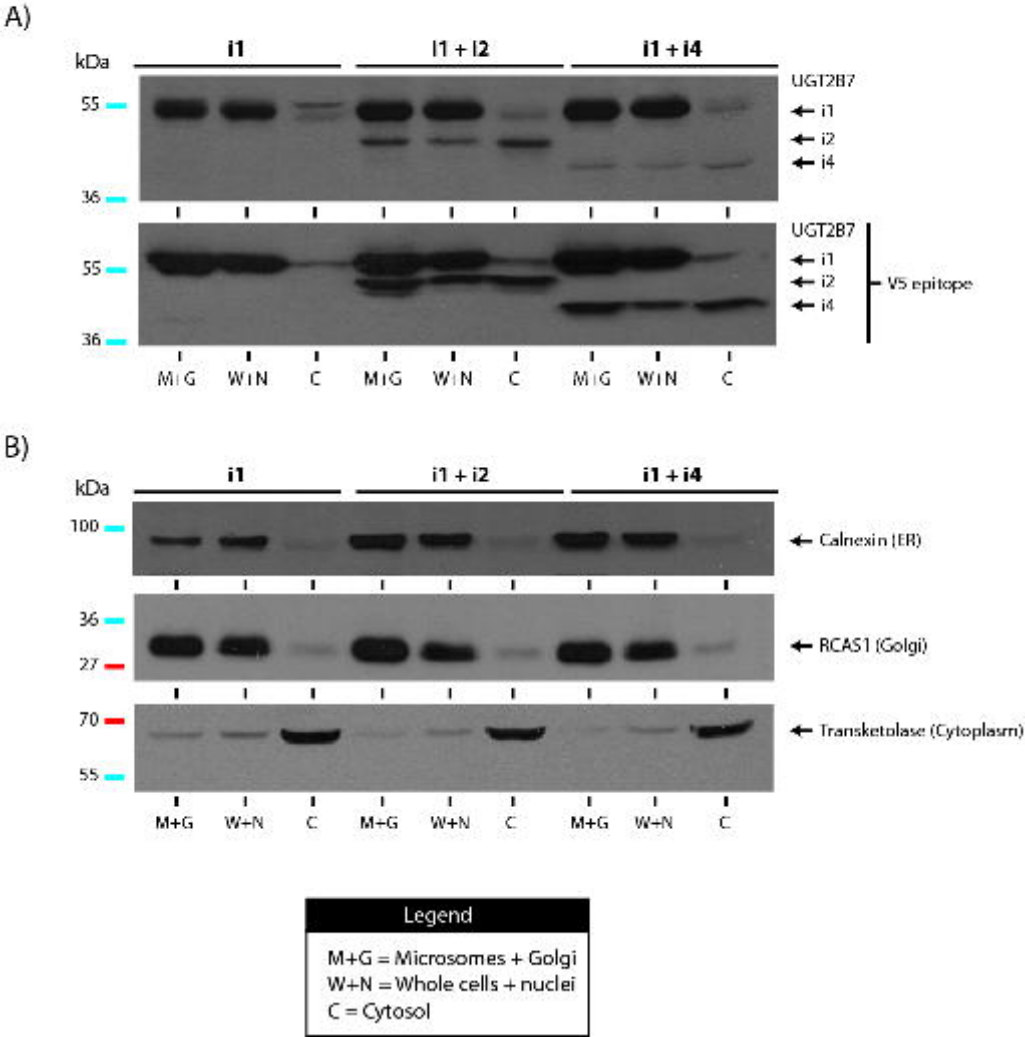
A)
kDa
i1
I1 + I2
i1 + i4
55
36
UGT2B7
← i1
← i2
← i4
UGT2B7
← i1
← i2
← i4
V5 epitope
M+G
W+N
C
B)
kDa
i1
i1 + i2
i1 + i4
100
36
27
70
55
← Calnexin (ER)
← RCAS1 (Golgi)
← Transketolase (Cytoplasm)
M+G
W+N
C
Legend
M+G = Microsomes + Golgi
W+N = Whole cells + nuclei
C = Cytosol

Figure 5

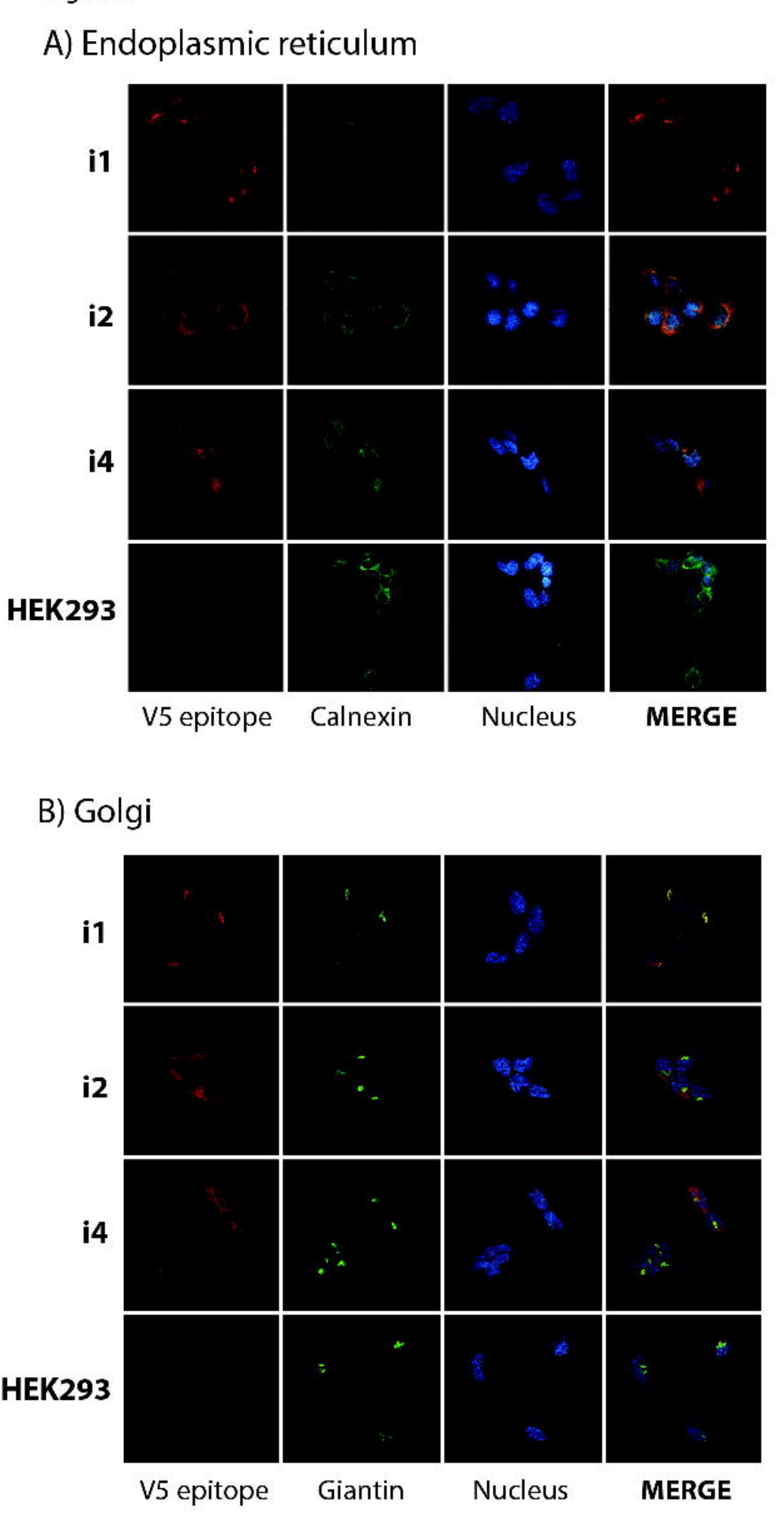
A) Endoplasmic reticulum
i1
i2
i4
HEK293
V5 epitope
Calnexin
Nucleus
MERGE
B) Golgi
i1
i2
i4
HEK293
V5 epitope
Giantin
Nucleus
MERGE

Figure 6

A)

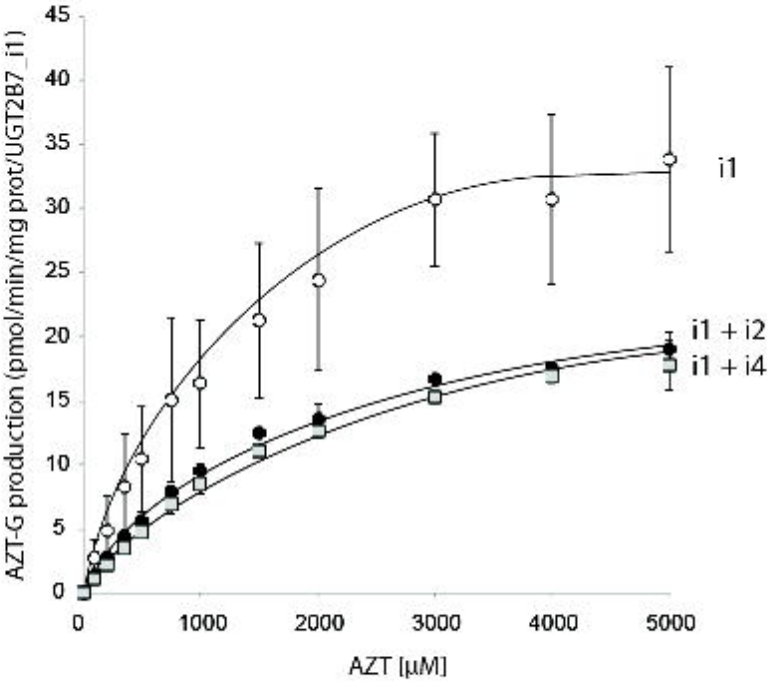

UGT2B7 clonal cells	Relative Vmax pmol/min/mg/i1 levels	Apparent Km µM
i1	44.5 ± 4.6	1550 ± 392
i1 + i2	25.2 ± 0.5 *	1635 ± 96
i1 + i4	25.1 ± 0.8 *	2022 ± 147

B)

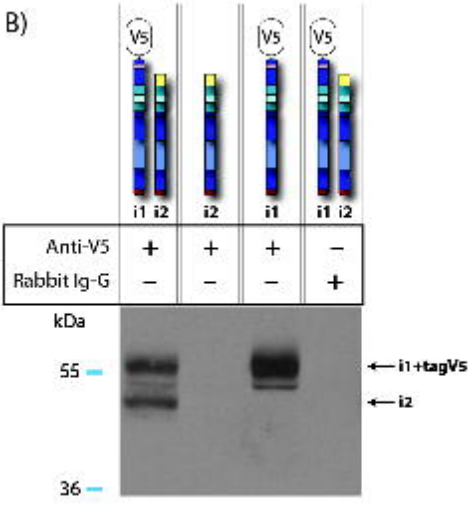

C)

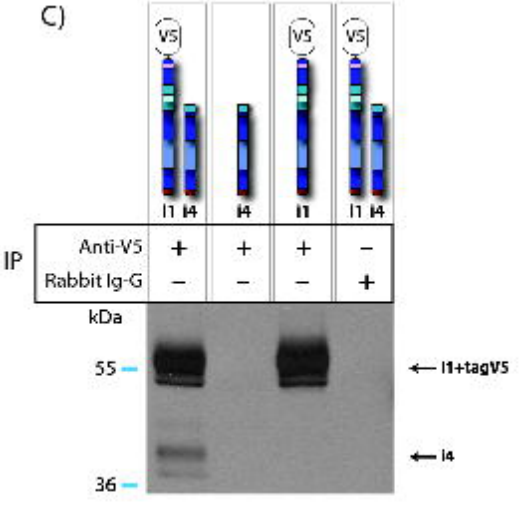

Figure 7

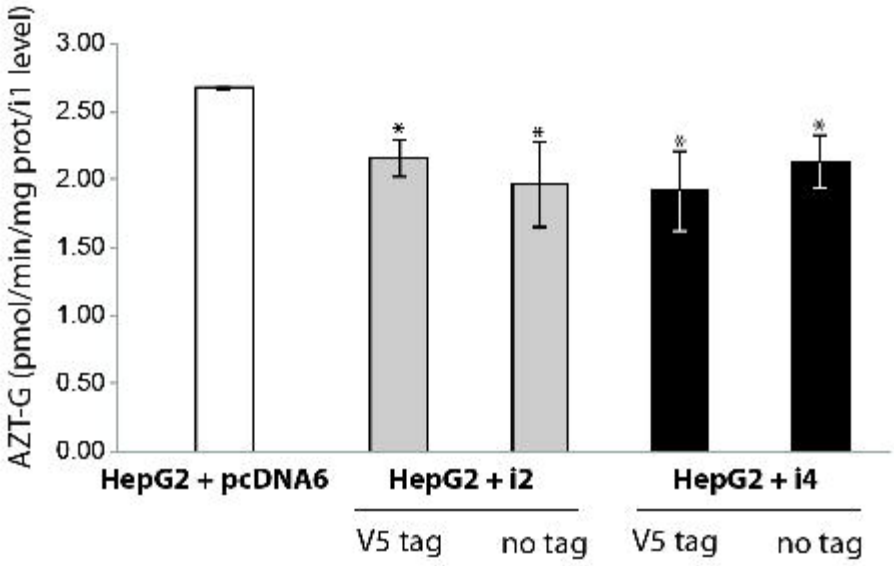

Occurence of alternative splicing events
(Splicing events/10^4 36B4 copies)

Ex5 - Ex6b	6 ± 2	7195 ± 209	7455 ± 272	6 ± 1	7 ± 1
Ex4 - Ex6a	7 ± 1	8 ± 1	22 ± 6	286 ± 36	800 ± 64
Ex5 - Ex6a	614 ± 16	668 ± 69	1089 ± 33	527 ± 51	535 ± 39

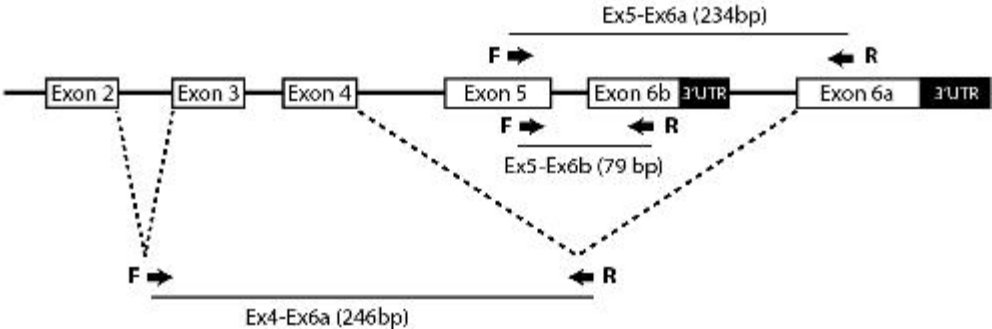

Figure 8

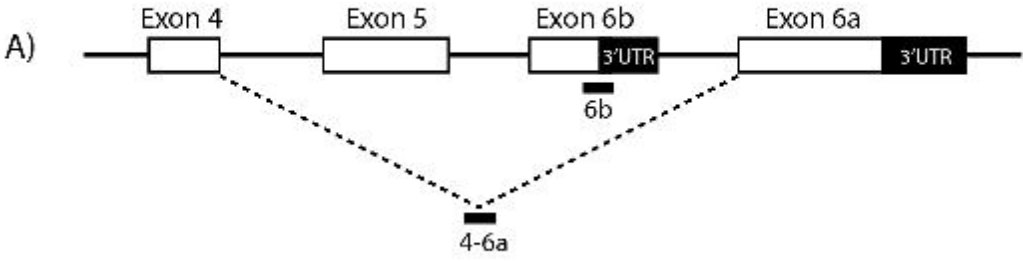
A)
Exon 4
Exon 5
Exon 6b
Exon 6a
3'UTR
3'UTR
6b
4-6a

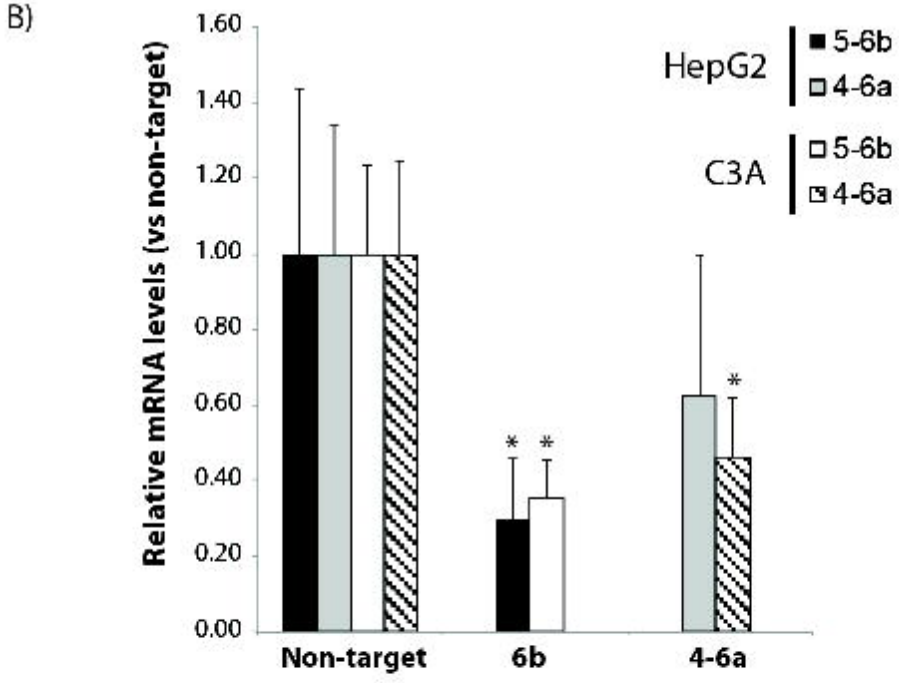
B)
Relative mRNA levels (vs non-target)
1.60
1.40
1.20
1.00
0.80
0.60
0.40
0.20
0.00
HepG2
5-6b
4-6a
C3A
5-6b
4-6a
*
*
*
Non-target
6b
4-6a

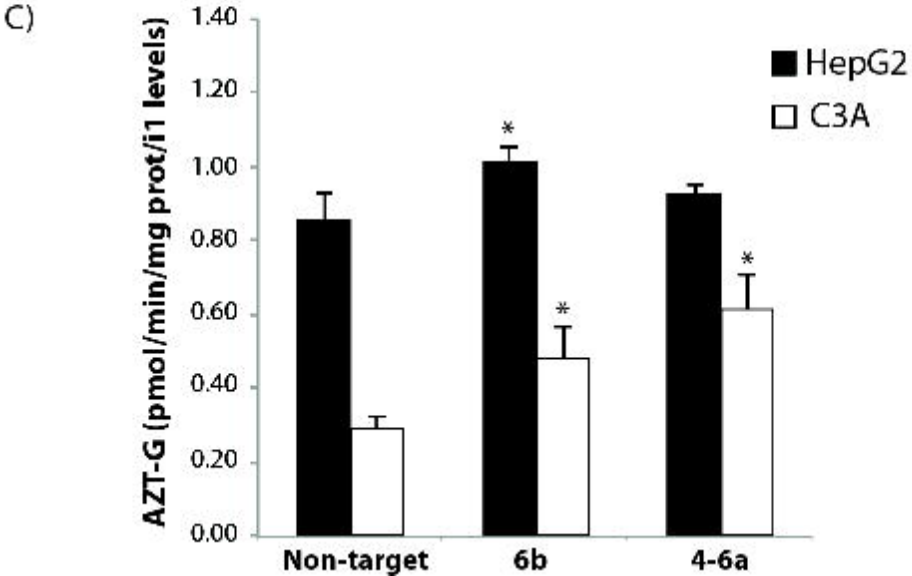
C)
AZT-G (pmol/min/mg prot/i1 levels)
1.40
1.20
1.00
0.80
0.60
0.40
0.20
0.00
HepG2
C3A
*
*
*
Non-target
6b
4-6a